

A high-velocity star recently ejected by an intermediate-mass black hole in M15

Yang Huang^{1,3,7,†,✉}, Qingzheng Li^{2,1,†}, Jifeng Liu^{3,1,7,✉}, Xiaobo Dong^{2,✉}, Huawei Zhang^{5,6,✉}, Youjun Lu^{1,4}, Cuihua Du¹

¹School of Astronomy and Space Science, University of Chinese Academy of Sciences, Beijing 100049, People's Republic of China;

²Yunnan Observatories, Chinese Academy of Sciences, Kunming 650011, China;

³New Cornerstone Science Laboratory, National Astronomical Observatories, Chinese Academy of Sciences, Beijing 100012, China;

⁴National Astronomical Observatories, Chinese Academy of Sciences, Beijing 100012, China;

⁵Department of Astronomy, School of Physics, Peking University, Beijing 100871, China;

⁶Kavli Institute for Astronomy and Astrophysics, Peking University, Beijing 100871, China;

⁷Institute for Frontiers in Astronomy and Astrophysics, Beijing Normal University, Beijing, 102206, China;

† These authors contributed equally;

✉ Corresponding authors: jfliu@nao.cas.cn; huangyang@ucas.ac.cn; xbdong@ynao.ac.cn; zhanghw@pku.edu.cn.

Abstract

The existence of intermediate-mass black holes (IMBHs) is crucial for understanding various astrophysical phenomena, yet their existence remains elusive, except for the LIGO-Virgo detection. We report the discovery of a high-velocity star J0731+3717, whose backward trajectory about 21 Myr ago intersects that of globular cluster M15 within the cluster tidal radius. Both its metallicity [Fe/H] and its alpha-to-iron abundance ratio [α /Fe] are consistent with those of M15. Furthermore, its location falls right on the fiducial sequence of the cluster M15 on the color-absolute magnitude diagram, suggesting similar ages. These support that J0731+3717 is originally associated with M15 at a confidence level of “seven nines”. We find that such a high-velocity star ($V_{ej} = 548_{-5}^{+6}$ km s⁻¹) was most likely tidally ejected from as close as one astronomical unit to the center of M15, confirming an IMBH ($\geq 100M_{\odot}$ with a credibility of 98%) as the exclusive nature of the central unseen mass proposed previously.

Keywords: Intermediate-mass black hole, Hills mechanism, hypervelocity star, globular cluster, large-scale survey

Introduction

Intermediate-mass black holes (IMBHs) in the mass range of 10^2 – 10^5 solar mass (M_{\odot}) may fill the gap between the BHs formed as stellar remnants and the supermassive BHs (SMBHs) found in the centers of galaxies¹. Except for LIGO-Virgo

detection^{2,3}, their existence, however, is still uncertain despite extensive searching efforts. Discovering IMBHs and characterizing their mass function in this range are thus of great interest for many reasons¹.

Globular clusters (GCs), dense and massive dynamical systems, have long been expected as promising places to harbor IMBHs. Both theory and numerical simulations suggest that IMBHs can form either through the repeated mergers of stellar black holes (“slow mode”)⁴, remnants of massive stars that sink to the center, or through the explosion of a very massive star resulting from runaway mergers of stars during an early phase of cluster core collapse (“fast mode”)⁵. The “slow mode” is a competitive scenario to explain the LIGO-Virgo detected IMBHs^{2,3}, yielded from mergers of binary BHs.

Extensive efforts have indeed found a large central unseen mass in some globular clusters by velocity dispersion^{6,7} or pulsar timing measurements⁸, but such a mass can be either an IMBH or a cluster of stellar remnants within a few thousand astronomical unit (AU)^{9–11}. To exclude the latter possibility, we need to limit the central mass to a much smaller volume. One approach is to search for hyper/high-velocity stars ejected from globular clusters. If they exist, they are largely linked to the tidal interaction between an IMBH and a binary system for a close encounter typically within one AU.

Results and Discussion

A high-velocity star ejected from globular cluster M15

To discover high-velocity stars ejected from globular clusters, backward orbital integrations are carried for 934 high-velocity ($V_{GSR} \geq 400$ km s⁻¹) halo stars in the searching volume within 5 kpc from the Sun¹² and 145 Galactic globular clusters^{13–15}. Both trajectories of stars and globular clusters are traced back to 250 Myr ago (in about one orbital period at solar position) using a common-adopted model of steady-state Galactic potential¹⁶. The closest distance for each pair of high-velocity star and globular cluster is calculated from their backward trajectories. Amongst the hundred thousand pairs, only J0731+3717 has closest distance smaller than the tidal radius of M15, making it a rare candidate of cluster ejected high-velocity star (More technical details can be found in Supplementary Materials A to F).

Table 1 summarizes the information of J0731+3717 and M15. J0731+3717 is a high-velocity star with $V_{GSR} = 419_{-6}^{+6}$ km s⁻¹ at a heliocentric distance of 1.295 ± 0.013 kpc. M15 is a 12.5 billion year old globular cluster¹⁷ located at the constellation Pegasus with a heliocentric distance of $10.71 \pm$

Table 1 – The measured parameters of J0731+3717 and M15

Parameter	J0731+3717	M15	Units
RA (J2000)	07:31:27.26	21:29:58.33	hh:mm:ss.ss
Dec (J2000)	+37:17:04.3	+12:10:01.2	dd:mm:ss.s
<i>Gaia</i> DR3 source_id	898707303799931392	n.a.	n.a.
<i>Gaia</i> DR3 Proper motion $\mu_{\alpha \cos \delta}$	47.963 ± 0.041	-0.659 ± 0.024	mas yr ⁻¹
<i>Gaia</i> DR3 Proper motion μ_{δ}	-83.666 ± 0.035	-3.803 ± 0.024	mas yr ⁻¹
<i>Gaia</i> DR3 Parallax	0.733 ± 0.042	0.097 ± 0.010	mas
<i>Gaia</i> DR3 <i>G</i> -band magnitude	15.814 ± 0.003	n.a.	mag
<i>Gaia</i> DR3 $G_{BP} - G_{RP}$	0.765 ± 0.007	n.a.	mag
SDSS <i>u</i> -band magnitude	17.095 ± 0.008	n.a.	mag
SDSS <i>g</i> -band magnitude	16.194 ± 0.004	n.a.	mag
SDSS <i>r</i> -band magnitude	15.832 ± 0.004	n.a.	mag
SDSS <i>i</i> -band magnitude	15.693 ± 0.004	n.a.	mag
SDSS <i>z</i> -band magnitude	15.643 ± 0.007	n.a.	mag
Distance	1295.2 ± 13.1	10709.0 ± 95.5	pc
$E(B - V)$	0.047	0.08	mag
Heliocentric radial velocities HRV	196.68 ± 6.97	-107.0 ± 0.2	km s ⁻¹
Effective temperature T_{eff}	6062.0 ± 157.0	n.a.	K
Surface gravity $\log g$	4.02 ± 0.29	n.a.	dex
Metallicity [Fe/H]	-2.23 ± 0.13	-2.33 ± 0.02 (stat.) ± 0.10 (syst.)	dex
α -element to iron ratio [α/Fe]	$+0.24 \pm 0.07$	0.24 ± 0.03	dex
Total velocity V_{GSR}	$418.71^{+6.54}_{-5.95}$	$111.85^{+1.48}_{-1.35}$	km s ⁻¹
Age	$13.00^{+1.75}_{-2.00}$	12.5 ± 0.3	Gyr
Mass	$0.69^{+0.02}_{-0.01}$	4.94×10^5	M_{\odot}

0.10 kpc¹⁴ and a mass of $5 \times 10^5 M_\odot$ ¹⁸. M15 is believed to host an intermediate-mass black hole (IMBH) of 1700–3200 M_\odot based on velocity dispersion measurements^{6,19}, albeit with debates^{9,20,21}, especially the 3σ upper limit of 980 M_\odot placed by the non-detection from ultra-deep radio observations at the cluster core²². While J0731+3717 is currently 11.5 kpc away from M15, their backward trajectories intersect with each other 21 Myr ago with a relative velocity of 548_{-5}^{+6} km s⁻¹ and a closest distance of 58 pc (Figure 1a), smaller than the cluster tidal radius of 132 pc. The intersection locations and their uncertainties in 3D space are estimated with one million Monte Carlo (MC) trajectory simulations to be $\Delta X = 20_{-135}^{+122}$ pc, $\Delta Y = 19_{-104}^{+95}$ pc and $\Delta Z = 51_{-32}^{+32}$ pc, as shown in Figures 1b-d.

In addition to the orbital connection, J0731+3717 exhibits rare chemical fingerprints consistent with those of M15. The SEGUE spectrum²³ clearly shows J0731+3717 is a very metal-poor late F-type star, as plotted in Figure 2a, with effective temperature $T_{\text{eff}} = 6062 \pm 157$ K, metallicity $[\text{Fe}/\text{H}] = -2.23 \pm 0.13$ and alpha-to-iron abundance ratio $[\alpha/\text{Fe}] = +0.24 \pm 0.07$ (see Supplementary Materials E). The old globular cluster M15 has well-measured $[\text{Fe}/\text{H}] = -2.33 \pm 0.10$ and $[\alpha/\text{Fe}] = +0.24 \pm 0.03$ ^{24,25}. Their chemical parameters are consistent with each other within errors, and are both located in a region with very few stars on the $[\text{Fe}/\text{H}]$ – $[\alpha/\text{Fe}]$ plane. Only 7.5×10^{-3} of all halo stars within the 5 kpc searching volume having reliable abundances are located in such a region shown in Figure 2b. The rare chemical similarity implies J0731+3717 was originally associated with the cluster, in line with the suggestion of orbital analysis.

The association of J0731+3717 with M15 can be further supported by their similar ages as derived from isochrone fitting. Broad-band photometric measurements for M15 and J0731+3717 are adopted from the Sloan Digital Sky Survey (SDSS) Galactic globular and open clusters project²⁶ and SDSS DR12²⁷, respectively. Both their absolute magnitudes and colors are corrected for extinction values along their separate lines of sight. As shown in Figure 2c, J0731+3717 falls right on the cluster fiducial sequence of M15; subsequently, its isochrone age as estimated from Bayesian approach is $13.00_{-2.00}^{+1.75}$ Gyr, almost identical to the age obtained for M15 (see Supplementary Materials F and G). In comparison, 37% of the field halo stars with chemical abundances similar to M15 (defined by the box in Figure 2b) actually deviate from its fiducial sequence by more than 0.05 mag (the maximal error) in color direction, implying significantly different ages.

It is extremely unlikely for the association of J0731+3717 and M15 to be by pure chance, given the probability for random association, chemical and age similarities. To quantitatively determine the probability of random high-velocity halo stars to encounter M15, we run MC simulations to generate about one million high-velocity halo stars with $V_{\text{GSR}} \geq 400$ km s⁻¹ in such a searching volume (see Supplementary Materials H). Only 12 high-velocity stars have close encounters with M15 within its tidal radius in the past 250 Myr. This means the probability of unphysical orbital encounter between J0731+3717 and M15 is 1.2×10^{-5} . Considering the orbital link, together with

the chemical and age similarities, one high-velocity halo star in our searching volume is coincidentally linked to M15 by a pure chance of only 5.89×10^{-8} . In other words, J0731+3717 is a true former member of M15 at a confidence level of “seven nines”.

Interpretation as Hills ejection via IMBH

An energetic ejection mechanism is required to kick-off J0731+3717 from M15 with an ejection velocity up to 548_{-5}^{+6} km s⁻¹; in comparison, the cluster central escape velocity is only 62 km s⁻¹ (the escape velocity at the cluster half-mass radius is 27 km s⁻¹; ref.²⁸). The Hills mechanism²⁹ invokes three-body exchange interactions between stellar binary and super-massive BHs to eject hypervelocity stars from the Galactic center; such a mechanism can naturally eject high-velocity stars from the IMBHs in the center of globular clusters. If this mechanism is at work in this case, the ejection velocity would constrain the mass of central BH in M15 to be 726 M_\odot for a binary separation $a = 0.05$ AU and 5804 M_\odot for $a = 0.10$ AU. A stellar-mass BH smaller than 100 M_\odot can also eject a star up to around 550 km s⁻¹ if $a \leq 0.025$ AU, but the probability is only few percent based on our MC simulations of two hundred million Hills ejections (see Supplementary Materials I and Figure 3). Thus, the ejection of J0731+3717 from M15 requires an IMBH ($\geq 100 M_\odot$ with a credibility of 98%) at the center of the cluster; the encounters mostly occurred (93%) within 2 AU from the cluster center. This confirms that the previously claimed aggregated mass of more than a few thousand solar mass^{6,19,22} is indeed an IMBH rather than a cluster of stellar remnants^{20,21}.

Excluding alternative explanations

A competing mechanism to eject high-velocity stars (even up to 2000 km s⁻¹) in globular cluster is the single star-binary interaction involving compact objects. Observations reveal the presence of a binary neutron star possibly as remnant from these encounters in M15³⁰. However, the ejection rate, as derived by a recent comprehensive Monte Carlo N-body simulation³¹, for producing J0731+3717 like high-velocity stars remains remarkably low, approximately 4×10^{-8} yr⁻¹ at present-day, which is three orders of magnitude lower than that of aforementioned IMBH–binary encounters (see Supplementary Materials J). The same simulation shows that no J0731+3717 like high-velocity stars with $V_{\text{GSR}} \geq 400$ km s⁻¹ were kicked from M15 through this channel in the past 10 Gyr (let alone the past 250 Myr).

High ejection velocity can be obtained through several alternative scenarios. First, a star can be kicked through normal single star-binary interaction³² without compact objects involved or exchange collision with a massive star³³ (similar to Hills mechanism but for massive stars), but the typical ejection velocity is within 200 km s⁻¹. To kick-off a J0731+3717 like star with ejection velocity above 550 km s⁻¹, interaction between a very massive star (50–100 M_\odot) and a hard massive binary is required³³, which is impossible to happen in such an old cluster M15 most recently. Second, a star can be ejected by the core-collapse supernova explosion of its former massive companion in a binary scenario³⁴. However, this is unlikely occurred recently in the old cluster M15 and the maximum kick velocity is largely within 300–400 km s⁻¹³⁵. At present, only the type Ia supernovae from the white dwarf plus helium star (hot

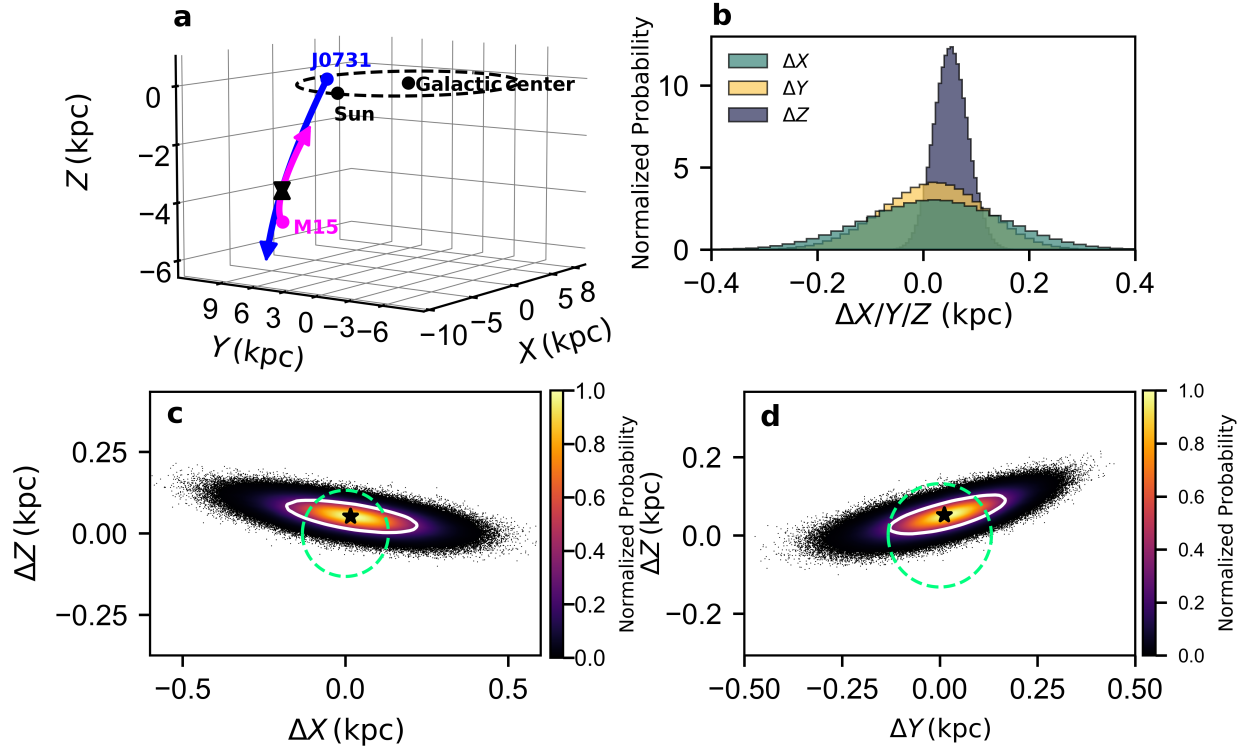


Figure 1 – Backward orbital analysis of J0731+3717 and M15. **a**, 3D representation of the backward orbits of J0731+3717 and the globular cluster M15. The blue and magenta lines with arrows mark the backward orbits of J0731+3717 and M15, respectively. The triangle and inverted triangle mark the encounter positions, happened 21 Myr ago, for M15 and J0731+3717. The black dots represent the locations of the Galactic center and the Sun as labelled. The solar circle ($R = 8.178$ kpc) is shown by the dashed black line. **b**, The distributions of the closest distance between J0731 and the center of M15 along X (green), Y (yellow) and Z (purple) at encounter yielded by one million MC trajectory simulation (see Supplementary Materials B). **c/d**, Density of the relative positions (J0731+3717 with respect to M15) at encounter, again yielded by the one million MC trajectory calculations, on (c) ΔX - ΔZ and (d) ΔY - ΔZ planes. The normalized number density is color coded, as shown by the right colorbar. The white contours mark 1σ confidence region. The green dashed circles represent the size of tidal radius of M15. The black star represent the relative location at closest distance derived directly using the observational parameters listed in Table 1.

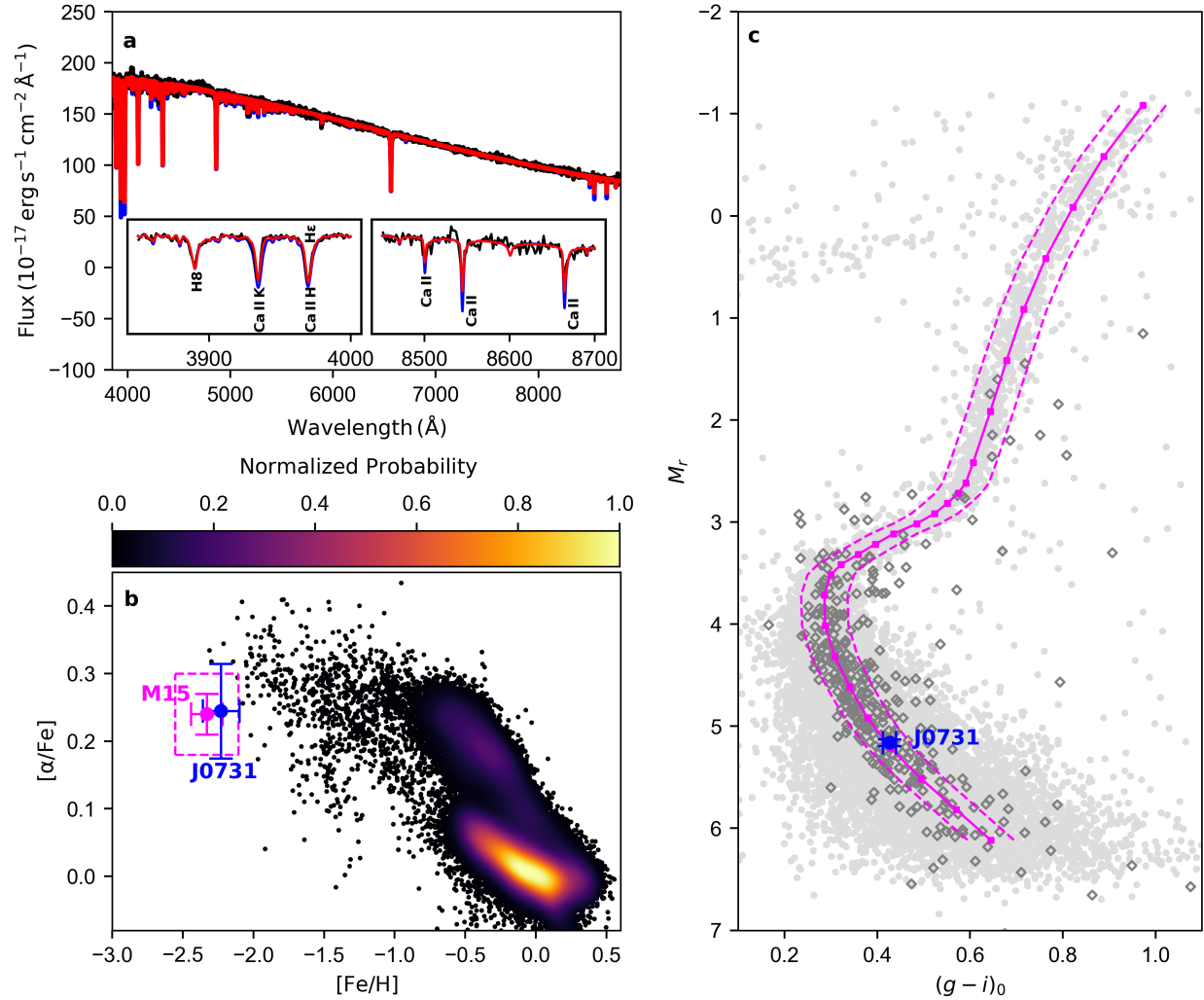


Figure 2 – Optical spectrum, chemical properties and color-absolute magnitude diagram of J0731+3717 and M15. **a**, Optical spectrum (in black) of J0731+3717 from the SEGUE survey. Two synthetic spectra (degraded to SEGUE spectral resolution) are overplotted for comparisons (see Supplementary Materials E). The red one has stellar parameters ($T_{\text{eff}} = 6100$ K, $\log g = 4.0$, $[\text{Fe}/\text{H}] = -2.0$ and $[\alpha/\text{Fe}] = +0.20$) similar to those of J0731+3717, while the blue one is 0.5 dex richer in metallicity (i.e. $[\text{Fe}/\text{H}] = -1.5$) with the other parameters unchanged. The insets zoom in the regions of Ca II H ($\lambda 3968$) and K ($\lambda 3933$) lines, and Ca II triplet lines at $\lambda\lambda 8498$, 8542, 8662. **b**, $[\text{Fe}/\text{H}]$ – $[\alpha/\text{Fe}]$ diagram for J0731+3717 (blue dot) and globular cluster M15 (magenta dot). The dashed magenta box marks the region within two times of measurement uncertainties of $[\text{Fe}/\text{H}]$ and $[\alpha/\text{Fe}]$ for M15. For comparison purpose, the background shows the density of APOGEE targeted stars with reliable determinations of $[\text{Fe}/\text{H}]$ and $[\alpha/\text{Fe}]$ (see Supplementary Materials H). **c**, M_r versus $(g-i)_0$ diagram of globular cluster M15 and J0731+3717. The background gray dots are photometric observations of M15 from the Sloan Digital Sky Survey Galactic globular and open clusters project²⁶, by adopting a cluster distance of 10.71 kpc and an $E(B-V)$ value of 0.08 (Table 1). The magenta squares denote the cluster fiducial sequence that is derived from the background gray dots by ref.²⁶. The dashed magenta lines are shifted from the fiducial sequence by ± 0.05 mag in $(g-i)_0$. The diamonds are field halo stars from the existing spectroscopic surveys with chemical fingerprints (defined by the magenta box shown in panel b) similar to M15 (see Supplementary Materials H).

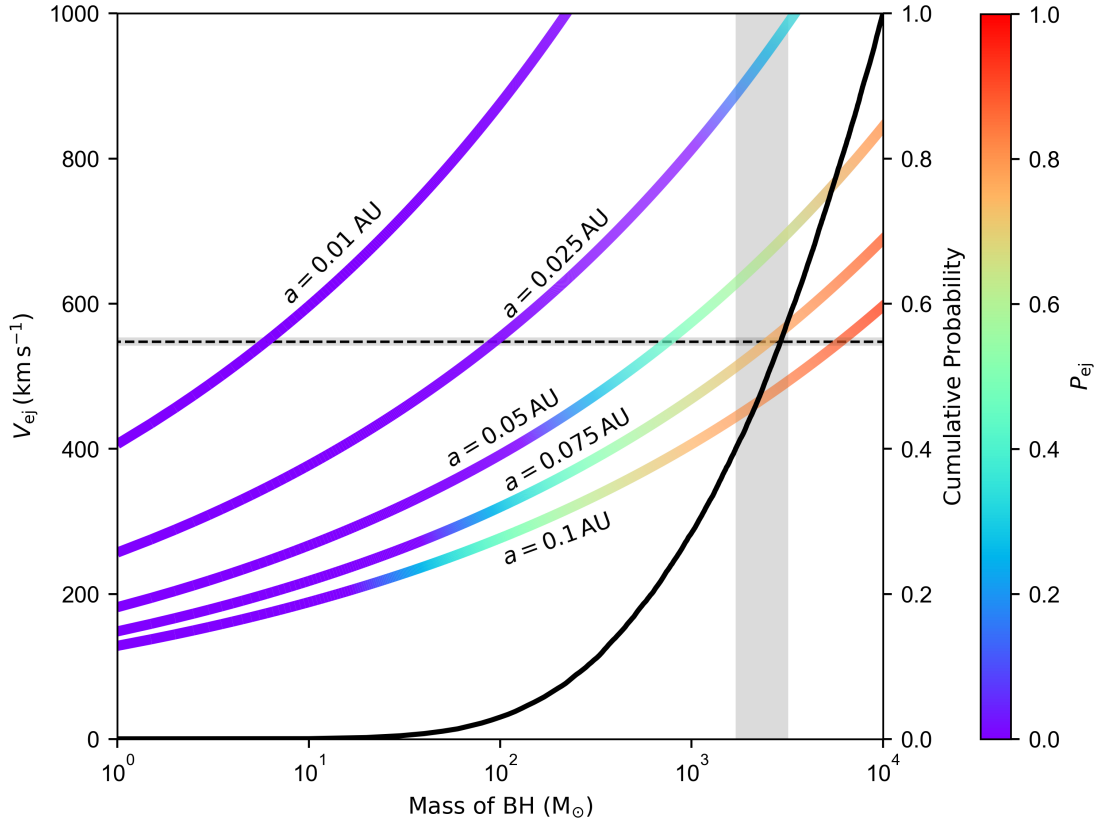


Figure 3 – Ejection velocities predicted by Hills mechanism. The lines represent the most probable ejection velocities, calculated by Equation S7 in Supplementary Materials I, as a function of black hole mass under different binary separation ranging from 0.01 to 0.1 AU (from left to right). In the calculation, the binary is assumed to contain two J0731+3717 like stars, each with a mass of $0.69M_{\odot}$. The color of lines indicates the ejection probability derived from Equation S9 in Supplementary Materials I with the colorbar shown on the right side. Here the closest distance that the binary can approach to the black hole is set to 0.5 AU. The horizontal dashed line with a shaded 1σ uncertainty indicates the reported ejection velocity ($548^{+6}_{-5} \text{ km s}^{-1}$) of J0731+3717. The vertical shaded region represents the mass of black hole ($1700\text{-}3200 M_{\odot}$) of M15 dynamically derived from velocity dispersion measurements^{6,19}. The black line represents the cumulative probability of the ejection of 0731+3717-like stars at different masses of black holes, calculated through Monte Carlo simulations (see Supplementary Materials I).

subdwarf) or the dynamically driven double-degenerate double-detonation^{36,37} channels can eject the surviving helium star or white dwarf with velocity even up to 1000 km s^{-1} like US 708³⁸ or like D6-1 to D6-3³⁷. One possible such ejection associated with the GC was recently reported in the nearby galaxy NGC 5353³⁹. The late F-type nature of J0731+3717 certainly rules out the possibility of a fast helium star or white dwarf ejected by the type Ia supernovae explosion. Third, a star can be stripped from the cluster when the latter experiences tidal shock from interactions with giant molecular clouds⁴⁰, Galactic disk⁴¹, spiral arm⁴² or perigalactic passages⁴¹. Apparently, J0731+3717 is not such a case since the ejection position (at -3.6 kpc below the Galactic disk plane; see Figure 1a) is far away from the Galactic disk, known giant molecular clouds or the last pericenter of M15. In summary, the above alternative ejection mechanisms are not viable to kick-off J0731+3717 from M15.

Conclusion

Our discovery of J0731+3717 ejected by an IMBH in M15 thus proves that the existence of IMBHs can be disclosed by high-velocity stars ejected from clusters via Hills mechanism, unambiguously as compared to previous velocity dispersion measurements^{6,9,20,21}. Such a method can be applied to find more cases like J0731+3717 in our Galaxy. Simulations of the 145 globular clusters in the past 14 Gyr led to around 500 J0731+3717 like high-velocity stars ejected into the current 5 kpc searching volume (see Supplementary Materials J, although only 50 of them were ejected in the past 250 Myr that can be traced back to their cluster origin under current measurement uncertainties. With the increasing power of ongoing *Gaia* and large-scale spectroscopic surveys, we expect to discover dozens of cases within the 5 kpc volume and ten times more within a 10 kpc volume, which should shed light on the understanding of the evolutionary path from stellar-mass BHs to SMBHs.

Methods

Detailed methods are available in the Supplementary data.

Data Availability

All data used in this study is publicly available. This work made use of data from the European Space Agency (ESA) mission *Gaia* (<https://www.cosmos.esa.int/gaia>), processed by the Gaia Data Processing and Analysis Consortium (DPAC, <https://www.cosmos.esa.int/web/gaia/dpac/consortium>). The stellar parameters of J0731+3717 is available from the SDSS-II/III SEGUE archive at <https://data.sdss.org/sas/dr12/sdss/sspp/ssppOut-dr12.fits>. The SDSS photometric and spectroscopic data can be found at <http://skyserver.sdss.org/dr12/en/tools/search/radial.aspx>. The photometric catalog of M15 is available from http://das.sdss.org/va/osuPhot/v1_0/. The stellar isochrones can be found at <http://stellar.dartmouth.edu/models>. The data supporting the plots in this paper and other findings of this study are available from the corresponding authors upon reasonable request.

Code Availability

We use standard data analysis tools in the Python environments. Specifically, the orbital analysis is carried out with Python package *Gala* and *galpy*, which is publicly available at http://gala.adrian.pw/en/v1.6.1/getting_started.html and www.galpy.org.

Supplementary Data

Supplementary data are available at *NSR* online.

Acknowledgements

This work presents results from the European Space Agency (ESA) space mission *Gaia*. *Gaia* data are being processed by the Gaia Data Processing and Analysis Consortium (DPAC). Funding for the DPAC is provided by national institutions, in particular the institutions participating in the Gaia MultiLateral Agreement (MLA). The *Gaia* mission website is <https://www.cosmos.esa.int/gaia>. The *Gaia* archive website is <https://archives.esac.esa.int/gaia>.

Funding

This work is supported by the Strategic Priority Research Program of the Chinese Academy of Sciences (XDB0550103). Y.H. acknowledges the National Science Foundation of China (1242200163, 11903027 and 11833006), and the National Key RD Program of China (2023YFA1608303 and 2019YFA0405503). JFL acknowledges support the National Science Foundation of China (11988101 and 11933004), and support from the New Cornerstone Science Foundation through the New Cornerstone Investigator Program and the XPLOER PRIZE. X.B.D. acknowledges the support from the National Science Foundation of China (12373013). H.W.Z. acknowledges the National Science Foundation of China (11973001, 12090040 and 12090044), and the National Key RD Program of China (2019YFA0405504).

Author Contributions

Y.H. led this project and wrote the paper; Q.Z.L. contributed to the sample preparation, systematic search, data analysis, and wrote the manuscript together with Y.H.; J.F.L. contributed to the interpretation of the results and writing the text; H.W.Z. contributed to the project planning, discussions, and text revisions; X.B.D. contributed to the project planning, discussions, and text revisions; Y.J.L. contributed to the interpretation and revisions of the text; C.H.D. contributed to the interpretation and revisions of the text.

Reference

1. Greene, J. E., Strader, J. & Ho, L. C. Intermediate-Mass Black Holes. *ARA&A* **58**, 257–312 (2020). 1911.09678.
2. Abbott, R. *et al.* GW190521: A Binary Black Hole Merger with a Total Mass of $150 M_{\odot}$. *Phys. Rev. Lett.* **125**, 101102 (2020). 2009.01075.
3. Abbott, R. *et al.* GWTC-3: Compact Binary Coalescences Observed by LIGO and Virgo during the Second Part of the Third Observing Run. *Physical Review X* **13**, 041039 (2023). 2111.03606.

4. Miller, M. C. & Hamilton, D. P. Production of intermediate-mass black holes in globular clusters. *Mon. Not. R. Astron. Soc.* **330**, 232–240 (2002). [astro-ph/0106188](#).
5. Portegies Zwart, S. F. & McMillan, S. L. W. The Runaway Growth of Intermediate-Mass Black Holes in Dense Star Clusters. *Astrophys. J.* **576**, 899–907 (2002). [astro-ph/0201055](#).
6. Gerssen, J. *et al.* Hubble Space Telescope Evidence for an Intermediate-Mass Black Hole in the Globular Cluster M15. II. Kinematic Analysis and Dynamical Modeling. *Astron. J.* **124**, 3270–3288 (2002). [astro-ph/0209315](#).
7. Noyola, E., Gebhardt, K. & Bergmann, M. Gemini and Hubble Space Telescope Evidence for an Intermediate-Mass Black Hole in ω Centauri. *Astrophys. J.* **676**, 1008–1015 (2008). [0801.2782](#).
8. Kiziltan, B., Baumgardt, H. & Loeb, A. An intermediate-mass black hole in the centre of the globular cluster 47 Tucanae. *Nature* **542**, 203–205 (2017). [1702.02149](#).
9. van den Bosch, R., de Zeeuw, T., Gebhardt, K., Noyola, E. & van de Ven, G. The Dynamical Mass-to-Light Ratio Profile and Distance of the Globular Cluster M15. *Astrophys. J.* **641**, 852–861 (2006). [astro-ph/0512503](#).
10. Baumgardt, H. *et al.* No evidence for intermediate-mass black holes in the globular clusters ω Cen and NGC 6624. *Mon. Not. R. Astron. Soc.* **488**, 5340–5351 (2019). [1907.10845](#).
11. Freire, P. C. C. *et al.* Long-term observations of the pulsars in 47 Tucanae - II. Proper motions, accelerations and jerks. *Mon. Not. R. Astron. Soc.* **471**, 857–876 (2017). [1706.04908](#).
12. Li, Q.-Z. *et al.* On the Origins of Extreme Velocity Stars as Revealed by Large-scale Galactic Surveys. *Astron. J.* **166**, 12 (2023). [2207.04406](#).
13. Harris, W. E. A New Catalog of Globular Clusters in the Milky Way. *arXiv e-prints* arXiv:1012.3224 (2010). [1012.3224](#).
14. Baumgardt, H. & Vasiliev, E. Accurate distances to Galactic globular clusters through a combination of Gaia EDR3, HST, and literature data. *Mon. Not. R. Astron. Soc.* **505**, 5957–5977 (2021). [2105.09526](#).
15. Vasiliev, E. & Baumgardt, H. Gaia EDR3 view on galactic globular clusters. *Mon. Not. R. Astron. Soc.* **505**, 5978–6002 (2021). [2102.09568](#).
16. Bovy, J. galpy: A python Library for Galactic Dynamics. *Astrophys. J. Supp.* **216**, 29 (2015). [1412.3451](#).
17. VandenBerg, D. A., Denissenkov, P. A. & Catelan, M. Constraints on the Distance Moduli, Helium and Metal Abundances, and Ages of Globular Clusters from their RR Lyrae and Non-variable Horizontal-branch Stars. I. M3, M15, and M92. *Astrophys. J.* **827**, 2 (2016). [1607.02088](#).
18. Dalgleish, H. *et al.* The WAGGS project-III. Discrepant mass-to-light ratios of Galactic globular clusters at high metallicity. *Mon. Not. R. Astron. Soc.* **492**, 3859–3871 (2020). [2001.01810](#).
19. Gerssen, J. *et al.* Addendum: Hubble Space Telescope Evidence for an Intermediate-Mass Black Hole in the Globular Cluster M15. II. Kinematic Analysis and Dynamical Modeling [iA href="/abs/2002AJ...124.3270G"¿Astron. J. 124, 3270 (2002);iA¿] (2003). [astro-ph/0210158](#).
20. Baumgardt, H., Hut, P., Makino, J., McMillan, S. & Portegies Zwart, S. On the Central Structure of M15. *Astrophys. J.* **582**, L21–L24 (2003). [astro-ph/0210133](#).
21. McNamara, B. J., Harrison, T. E. & Anderson, J. Does M15 Possess an Intermediate-Mass Black Hole in Its Core? *Astrophys. J.* **595**, 187–194 (2003).
22. Strader, J. *et al.* No Evidence for Intermediate-mass Black Holes in Globular Clusters: Strong Constraints from the JVL. *Astrophys. J.* **750**, L27 (2012). [1203.6352](#).
23. Yanny, B. *et al.* SEGUE: A Spectroscopic Survey of 240,000 Stars with $g = 14$ –20. *Astron. J.* **137**, 4377–4399 (2009). [0902.1781](#).
24. Carretta, E., Bragaglia, A., Gratton, R., D’Orazi, V. & Lucatello, S. Intrinsic iron spread and a new metallicity scale for globular clusters. *Astron. Astrophys.* **508**, 695–706 (2009). [0910.0675](#).
25. Dias, B. *et al.* FORS2/VLT survey of Milky Way globular clusters. II. Fe and Mg abundances of 51 Milky Way globular clusters on a homogeneous scale. *Astron. Astrophys.* **590**, A9 (2016). [1603.02672](#).
26. An, D. *et al.* Galactic Globular and Open Clusters in the Sloan Digital Sky Survey. I. Crowded-Field Photometry and Cluster Fiducial Sequences in ugriz. *Astrophys. J. Supp.* **179**, 326–354 (2008). [0808.0001](#).
27. Alam, S. *et al.* The Eleventh and Twelfth Data Releases of the Sloan Digital Sky Survey: Final Data from SDSS-III. *Astrophys. J. Supp.* **219**, 12 (2015). [1501.00963](#).
28. Gnedin, O. Y. *et al.* The Unique History of the Globular Cluster ω Centauri. *Astrophys. J.* **568**, L23–L26 (2002). [astro-ph/0202045](#).
29. Hills, J. G. Hyper-velocity and tidal stars from binaries disrupted by a massive Galactic black hole. *Nature* **331**, 687–689 (1988).
30. Phinney, E. S. & Sigurdsson, S. Ejection of pulsars and binaries to the outskirts of globular clusters. *Nature* **349**, 220–223 (1991).
31. Cabrera, T. & Rodriguez, C. L. Runaway and Hypervelocity Stars from Compact Object Encounters in Globular Clusters. *Astrophys. J.* **953**, 19 (2023). [2302.03048](#).
32. Perets, H. B. & Šubr, L. The Properties of Dynamically Ejected Runaway and Hyper-runaway Stars. *Astrophys. J.* **751**, 133 (2012). [1202.2356](#).
33. Gvaramadze, V. V., Gualandris, A. & Portegies Zwart, S. On the origin of high-velocity runaway stars. *Mon. Not. R. Astron. Soc.* **396**, 570–578 (2009). [0903.0738](#).
34. Blaauw, A. On the origin of the O- and B-type stars with high velocities (the “run-away” stars), and some related problems. *Bull. Astron. Inst. Netherlands* **15**, 265 (1961).
35. Evans, F. A., Renzo, M. & Rossi, E. M. Core-collapse supernovae in binaries as the origin of galactic hyper-runaway stars. *Mon. Not. R. Astron. Soc.* **497**, 5344–5363 (2020). [2006.00849](#).
36. Wang, B. & Han, Z. Companion stars of type Ia supernovae and hypervelocity stars. *Astron. Astrophys.* **508**, L27–L30 (2009). [0911.3316](#).
37. Shen, K. J. *et al.* Three Hypervelocity White Dwarfs in Gaia DR2: Evidence for Dynamically Driven Double-degenerate Double-detonation Type Ia Supernovae. *Astrophys. J.* **865**, 15 (2018). [1804.11163](#).
38. Geier, S. *et al.* The fastest unbound star in our Galaxy ejected by a thermonuclear supernova. *Science* **347**, 1126–1128 (2015). [1503.01650](#).
39. Bregman, J. N., Gnedin, O. Y., Seitzer, P. O. & Qu, Z. A Type Ia Supernova near a Globular Cluster in the Early-type Galaxy NGC 5353. *Astrophys. J.* **968**, L6 (2024). [2405.09701](#).
40. Gieles, M. *et al.* Star cluster disruption by giant molecular clouds. *Mon. Not. R. Astron. Soc.* **371**, 793–804 (2006). [astro-ph/0606451](#).
41. Gnedin, O. Y. & Ostriker, J. P. Destruction of the Galactic Globular Cluster System. *Astrophys. J.* **474**, 223–255 (1997). [astro-ph/9603042](#).
42. Gieles, M., Athanassoula, E. & Portegies Zwart, S. F. The effect of spiral arm passages on the evolution of stellar clusters. *Mon. Not. R. Astron. Soc.* **376**, 809–819 (2007). [astro-ph/0701136](#).

Supplementary Materials for

A high-velocity star recently ejected from the globular cluster M15

Yang Huang^{1,3,†,✉}, Qingzheng Li^{2,1,†}, Jifeng Liu^{3,1,7,✉}, Xiaobo Dong^{2,✉}, Huawei Zhang^{5,6,✉}, Youjun Lu^{1,4}, Cuihua Du¹

¹School of Astronomy and Space Science, University of Chinese Academy of Sciences, Beijing 100049, People's Republic of China;

²Yunnan Observatories, Chinese Academy of Sciences, Kunming 650011, China;

³New Cornerstone Science Laboratory, National Astronomical Observatories, Chinese Academy of Sciences, Beijing 100012, China;

⁴National Astronomical Observatories, Chinese Academy of Sciences, Beijing 100012, China;

⁵Department of Astronomy, School of Physics, Peking University, Beijing 100871, China;

⁶Kavli Institute for Astronomy and Astrophysics, Peking University, Beijing 100871, China;

⁷Institute for Frontiers in Astronomy and Astrophysics, Beijing Normal University, Beijing, 102206, China;

† These authors contributed equally;

✉ Corresponding authors: jfliu@nao.cas.cn; huangyang@ucas.ac.cn; xbdong@ynao.ac.cn; zhanghw@pku.edu.cn.

arXiv:2406.00923v2 [astro-ph.GA] 16 Sep 2024

Supplementary Materials

A Coordinate systems.

We adopt two sets of coordinate systems: (1) a right-handed Cartesian coordinate system (X, Y, Z) , with X towards the direction opposite of the Sun, Y pointing to the direction of Galactic rotation, and Z in the direction of north Galactic pole; (2) a Galactocentric cylindrical system (R, ϕ, Z) , with R the projected Galactocentric distance increasing radially outwards, ϕ the azimuthal angle towards the direction of the Galactic rotation, and Z the same as that in the Cartesian system. The Sun is set to at $(R_0, Z_\odot) = (8.178, 0.025)$ kpc (ref.^{1,2}) and the circular velocity at the solar position is fixed to $V_c(R_0) = 220$ km s⁻¹ (ref.³). The solar motions with respect to the local standard of rest are set to $(U_\odot, V_\odot, W_\odot) = (7.01, 10.13, 4.95)$ km s⁻¹ (ref.⁴).

B Systematic Search.

By combing datasets of the RAVE DR5 (ref.⁵), SDSS DR12 (ref.⁶), LAMOST DR8 (ref.⁷), APOGEE DR16 (ref.⁸), GALAH DR2⁹, and *Gaia* DR3 (ref.¹⁰), a large sample of 943 high-velocity halo stars with total velocity $V_{\text{GSR}} \geq 400$ km s⁻¹ are constructed¹¹. The distances of those stars are first estimated from the parallax measurements provided by *Gaia* DR3 using a Bayesian approach¹¹. The distance estimates are further improved by adding constraints from SDSS optical colors and chemical information (i.e., metallicity and $[\alpha/\text{Fe}]$ from spectroscopic surveys) into the Bayesian analysis, which will be introduced in the latter section. Their 3D velocities are then calculated from the measured distances, proper motions again from *Gaia* DR3 and heliocentric radial velocities (HRV) provided by the aforementioned spectroscopic surveys, except for the SDSS survey, whose HRV is carefully re-determined by the LAMOST stellar parameter pipeline at Peking University (LSP3; ref.¹²) utilizing specific template of similar atmospheric parameters for each star (see technique details in latter section). Moreover, they have metallicities and alpha-to-iron abundance ratios well measured from their spectra. We perform a systematic search for high-velocity stars ejected from globular clusters. To do so, backward orbital integrations are carried for those 943 high-velocity halo stars and 145 Galactic globular clusters with well measured metallicities, distances, proper motions and HRVs (refs.^{21,22,23}). For the orbital analysis, we adopt the python package `Gala`¹³ with the Galactic potential setting to `MilkyWayPotential`³, which contains four components: a nucleus, a bulge, a disk, and a dark matter halo. In this study, we only concern recent ejections during the past 250 Myr since the dynamical effects (e.g., the dynamical friction¹⁴), that globular cluster experienced, are hard to be precisely considered in the backward orbital calculations. The trajectories are therefore traced back in time of 250 Myr with a time resolution of 1 kyr. To discover cluster ejected high-velocity candidates, the trajectories of each high-velocity star and globular clusters are carefully investigated by sorting the ratios between the closest orbital distances d_{min} and the tidal radii r_t of the clusters which can be found at <https://people.smp.uq.edu.au/HolgerBaumgardt/globular/parameter.html>. The final candidates are required to have the ratios (d_{min}/r_t) smaller than one and metallicity differences between the high-velocity stars and the clusters smaller than 0.2 dex. During this search, we identified J0731+3717 (the only one of 135,430 trajectory pairs), a high-velocity star has a close encounter with M15 within its tidal radius about 21 Myr ago. The closest orbital distance is $58.0_{-58.0}^{+117.4}$ pc, which is smaller than the tidal radius ($r_t = 132.1$ pc) of M15 (see Extended Data Table 1 for top 5 clusters sorted by ratios of d_{min}/r_t). The encounter occurred where J0731+3717 is located at $(X, Y, Z) = (-5.91_{-0.14}^{+0.13}, 7.19_{-0.10}^{+0.10}, -3.61_{-0.04}^{+0.04})$ kpc with $(V_X, V_Y, V_Z) = (-205.16_{-6.68}^{+6.07}, -305.94_{-6.85}^{+6.23}, 171.19_{-3.37}^{+3.06})$ km s⁻¹, and M15 is located at $(X, Y, Z) = (-5.93_{-0.03}^{+0.03}, 7.17_{-0.09}^{+0.09}, -3.66_{-0.03}^{+0.03})$ kpc with $(V_X, V_Y, V_Z) = (56.18_{-1.95}^{+2.15}, 103.13_{-1.26}^{+1.26}, -82.10_{-1.30}^{+1.38})$ km s⁻¹. At the closest approach, J0731+3717 had a relative velocity of $541.10_{-5.42}^{+5.96}$ km s⁻¹ with respect to M15 (see Extended Data Figure 1). The upper and lower uncertainties of these reported parameters from our orbital analysis come from 16 and 84 per cent percentiles of the probability distribution function (PDF) yielded by one million MC trajectory calculations. During the calculations, the astrometric parameters (except the parallax/distance) of J0731+3717 are assumed to multivariate Gaussian distributions with the correlation coefficients (taken from *Gaia* DR3) considered. The distance of J0731+3717 is assumed to follow the posterior PDF derived from our Bayesian analysis. The HRV of J0731+3717 is uncorrelated to astrometric parameters and thus assumed normally distributed. For M15, the uncertainties in positions, distance, proper motions and HRV are taken from refs^{22,23}. and are all assumed to follow normal distribution.

We note that the last cross with the disk is happened 2.6 Myr ago with the intersect positions at $(X_p, Y_p) = (-9.1, 0.9)$ kpc, far away from the Galactic center. This result clearly rules out the possibility of ejecting J0737+3717 from the supermassive BH at the Galactic center. In addition to the above 250 Myr orbital integrations, the whole past 14 Gyr (the age of universe) backward orbits of J0731+3717 and globular clusters, as well as the best-known dwarf galaxies (parameters are adopted from ref.¹⁵), are investigated. No other orbital links are found. The whole backward orbits of J0731+3717 are also provided as an online supplementary data.

C Orbital deflections.

During the backward orbital integrations, the deflections caused by encounters with field stars are ignored. We thus here evaluate this effect on orbital analysis. The deflection angle is defined as¹⁶:

$$\theta_{\text{defl}} = 2 \tan^{-1}(b_{90}/b), \quad (\text{S1})$$

where b is the distance of the close approach, and b_{90} is the 90° deflection radius that is given by:

$$b_{90} = \frac{G(m_1 + m_2)}{V_0^2}, \quad (\text{S2})$$

where m_1 and m_2 are the masses of two stars having close meet, V_0 is the relative speed. By assuming two solar-like stars with $V_0 = 300 \text{ km s}^{-1}$, the deflection angle is only about 0.039 arcsec for a 1 pc encounter. The Sun is expected to experience 1 pc encounter at a rate of $19.7 \pm 2.2 \text{ Myr}^{-1}$. During our orbital calculations with a total integration time of 250 Myr, the maximum deflection angle for solar-like stars at solar position is within 3.5 arcmin, which is much smaller than the tidal radius of M15 (42.4 arcmin for $r_t = 132 \text{ pc}$ at 10.7 kpc). In our case, the deflection angles of these halo stars are even much smaller, given their much lower spatial number density. Specifically, for J0731+3717 with typical $V_0 = 420 \text{ km s}^{-1}$, the deflection angle is smaller than 8.4 arcsec (0.44 pc at the distance of M15), even assuming a high encounter rate at solar position. This deflection angle is not only much smaller than the tidal radius of M15 or uncertainty of meet distance (see above section) but also significantly less than its half-light radius (one arcmin from ref.²¹). Thus, the orbital deflection has minor effects on our backward orbital analysis.

D Orbital analysis with alternative assumptions.

To show the robustness of our backward orbital reconstructions, we repeat the whole analysis by adopting alternative assumptions. In total, six tests are performed. In each test, only one assumption is changed and other parameters remain the same. First, we change the Galactic potential to `BovyMWPotential2014`³ consisting three components: a bulge, a disk, and a dark matter halo. In the second test, alternative values of solar motions respect to the local standard of rest $(U_\odot, V_\odot, W_\odot) = (11.10, 12.24, 7.25) \text{ km s}^{-1}$ are adopted¹⁸. In the third test, we use the circular velocity at the solar position $V_c(R_0) = 234.04 \text{ km s}^{-1}$ (ref.¹⁹). In the fourth test, the Galactocentric distance of the sun R_0 is changed to 8.34 kpc²⁰. For the fifth test, M15 is modelled as a moving potential with a Plummer profile, calculated by the `MovingObjectPotential` function implemented in `galpy` (ref.³). The size and mass of M15 is taken from ref.²³. Finally, we consider the effects from the potential of the Large Magellanic Cloud (LMC), by modelling it as a Plummer profile with a total mass of $1.38 \times 10^{11} M_\odot$ and a scale radius of 17.14 kpc (ref.²⁴). The sky positions, distances, proper motions and HRV of LMC are adopted from ref.²⁵. The moving potential of LMC is again calculated by `MovingObjectPotential`. We also include the dynamical friction on the LMC from the Milky Way by the `ChandrasekharDynamicalFrictionForce` function of `galpy`. The closest encounter distances as found by the above tests are all within 60 pc (see Table S2), smaller than the tidal radius ($r_t = 132.1 \text{ pc}$) of M15. The backward time of the meets are all around 21 Myr, in great consistency with our default result. The comprehensive tests show that the impact of alternative assumptions on the backward orbital analysis is negligible.

E SEGUE spectra and parameters of J0731+3717.

Two optical spectra of J0731+3717 have been obtained by the SEGUE survey²⁶ on 2000 November 29 and 2005 March 17, with a signal-to-noise-ratio (SNR) of 49.4 and 55.8, respectively. The spectra have covered the full optical range (3800-9200Å) with a resolving power of around 2000. Stellar parameters and heliocentric radial velocity (HRV) are derived from the observed spectra by the SEGUE Stellar Parameter Pipeline (SSPP)²⁷. The typical precisions are 157 K, 0.29 dex, 0.13 dex, 0.07 dex and 5 km s^{-1} for effective temperature T_{eff} , surface gravity $\log g$, metallicity $[\text{Fe}/\text{H}]$, alpha-to-iron abundance ratio $[\alpha/\text{Fe}]$, and heliocentric radial velocity (HRV), respectively^{27,28}. Two groups of stellar parameters are derived by SSPP from the two visits and they are consistent with each other very well, showing the robustness of the pipeline. We here adopt the stellar parameters and HRV (Table 1) measured from the spectrum with highest SNR, i.e. the one observed on 2005 March 17. The spectrum is shown in Fig. 2a. Clearly, the SEGUE spectrum indicates that J0731+3717 is a real very metal-poor star with $[\text{Fe}/\text{H}]$ down to -2 and even lower, directly shown by the comparisons with the synthetic spectra adopted from Göttingen spectral library²⁹ (see Figure 2b).

Given the metal-poor nature of J0731+3717, we re-estimate its HRV and uncertainty by using a specific metal-poor template. To do so, we adopted the LSP3 that is developed to derive HRVs from LAMOST/SEGUE like low resolution spectra using cross-correlating technique with ELODIE library³⁰ as template (degraded to SEGUE resolution). We note the SEGUE spectrum (observed on 2005 March 17) of J0731+3717 was corrected for a systematic offset of $+7.3 \text{ km s}^{-1}$ due to wavelength calibrations (ref.³¹; <https://www.sdss3.org/dr9/algorithms/wavelength.php>). For the template, we choose BD+023375 ($T_{\text{eff}} = 5944 \text{ K}$, $\log g = 3.97$ and $[\text{Fe}/\text{H}] = -2.29$; ref.³⁰) star included in the ELODIE library, whose atmospheric parameters are very close to these of J0731+3717. We then run LSP3 to the SEGUE spectrum of J0731+3717 and find its HRV of $196.68 \pm 6.97 \text{ km s}^{-1}$. The 1σ error is properly estimated using metal-poor stars with multiple observations in LAMOST. This uncertainty is slightly larger than the typical one (5 km s^{-1}) for normal metal-rich FGK stars but in great consistent with the independent check from metal-poor globular clusters (ref.²⁸). As mentioned in previous systematic search section, the HRVs of other high-velocity stars from SDSS DR12 are also re-determined by LSP3 in the above manner.

F Mass, age and improved distance of J0731+3717.

We determine the mass, age and improved distance of J0731+3717 by the common used Bayesian approach. In this approach, the PDF of the age, mass and absolute magnitudes is expressed as,

$$f(\tau, m, M_\lambda) = NP(\tau, m)\mathcal{L}(\tau, m), \quad (\text{S3})$$

where $\lambda = u, g, r, i, z$ and N is a normalization parameter that ensures $\iint f(\tau, m)d\tau dm = 1$. For $P(\tau, m)$, a uniform prior and a Salpeter initial mass function³² are assumed for age and mass, respectively. The likelihood function \mathcal{L} is obtained by,

$$\mathcal{L} = \prod_{i=1}^n \frac{1}{\sqrt{2\pi}\sigma_i} \times \exp(-\chi_i^2/2), \quad (\text{S4})$$

where

$$\chi_i^2 = \left(\frac{O_i - M_i(\tau, m)}{\sigma_i} \right)^2. \quad (\text{S5})$$

Here O_i represents the observational constraints from the intrinsic color $(g - i)_0$, absolute magnitudes M_λ and metallicity [Fe/H], M_i represents the model values from the stellar isochrones, taken from the Dartmouth Stellar Evolution Program (DSEP)³³, at a give τ and M . The total number of observed parameters is n , and σ_i is the uncertainty of the i th observed parameter. The intrinsic color $(g - i)_0$ of J0731+3717 is from SDSS photometry after correcting for the dust reddening. The five SDSS band absolute magnitudes are given by combination of SDSS photometry with reddening corrected and the distance of J0731+3717 measured from *Gaia* parallax. Here the value of the reddening is taken from the SFD map³⁴ (after correction of 14% systematics³⁵) and the extinction coefficients are adopted from ref.³⁵. The metallicity [Fe/H] is derived from the SEGUE spectra. The uncertainties of these observational constraints (as listed in Table 1) are well considered in the estimation. For the DSEP isochrones, a constant value +0.20 dex of $[\alpha/\text{Fe}]$, close to that measured for J0731+3717, is adopted.

The resulted PDFs yield a mass of $0.69_{-0.01}^{+0.02} M_\odot$, an age of $13.00_{-2.00}^{+1.75}$ Gyr for J0731+3717 and a weighted mean distance modulus of 10.56 ± 0.02 (corresponding to $d = 1295.2 \pm 13.1$ pc) from the five SDSS bands. We note this method is also adopted to improve the distance estimate of other high-velocity stars in previous section of systematic search. In Figure S2, we compare J0731+3717 to the DSEP isochrones on the $M_r - (g - i)_0$ diagram to show the robustness of the resulted parameters. The derived age of J0731+3717 agrees very well with that determined for M15.

G Color-absolute magnitude diagram of M15.

We adopt the photometric measurements from the Sloan Digital Sky Survey Galactic globular and open clusters project³⁶ to construct the color-absolute diagram of M15. This project presents precise photometry for 17 Galactic globular clusters and open clusters by using the DAOPHOT/ALLFRAME procedure^{37,38} that are developed for crowded fields. We select M15 member stars from the catalog yielded by the project using the following criteria: 1) stars are within 6 arcmin from the center of M15; 2) stars in *gri*-bands are required with DAOPHOT parameters: $|\text{sharp}| < 1$ and $\chi < 1.5 + 4.5 \times 10^{-0.4(m-16.0)}$; 3) stars have photometric uncertainties smaller than 0.2 mag in *gri*-bands. In total, over ten thousand stars are left from the above cuts. By adopting a cluster distance of 10.71 kpc (ref.²³) and a dust reddening of $E(B - V) = 0.08$ (ref.³⁹), the color-absolute magnitude is constructed for M15 (see grey dots in Figure 2c). We further convert the cluster fiducial sequence (the locus of the number density peaks, taken from ref.³⁶) on r versus $(g - i)$ plane to that on M_r versus $(g - i)_0$ plane, by adopting the cluster distance and reddening values. The results are shown in Figure 2c as the magenta squares.

H Confidence level of the ejection of J0731+3717 from M15.

We calculate the possibility that one high-velocity halo star (in the 5 kpc searching volume) is linked to M15 by pure chance. First, we generate 50 million stars randomly distributed in a local volume of $(5\text{kpc})^3$ from the Sun (similar to the searching volume of high-velocity stars¹¹) following velocity distributions of the local halo stars:

$$f(v_R, v_\phi, v_Z) = k \exp \left(-\frac{v_R^2}{2\sigma_R^2} - \frac{(v_\phi - \bar{v}_\phi)^2}{2\sigma_\phi^2} - \frac{v_Z^2}{2\sigma_Z^2} \right), \quad (\text{S6})$$

where $k = \frac{1}{(2\pi)^{3/2}\sigma_R\sigma_\phi\sigma_Z}$, $\bar{v}_\phi = +35.53 \text{ km s}^{-1}$, $\sigma_R = 150.57 \text{ km s}^{-1}$, $\sigma_\phi = 115.67 \text{ km s}^{-1}$ and $\sigma_Z = 86.67 \text{ km s}^{-1}$ (ref.⁴⁰). In total, around one million stars (964,630) are found at the high-velocity tail with $V_{\text{GSR}} \geq 400 \text{ km s}^{-1}$. We thus perform backward orbital analysis for those high-velocity halo stars and the globular cluster M15. The integration settings are the same as those detailed in systematic search section. During the calculations, only 12 mock high-velocity halo stars have the chances to meet M15 within its tidal radius ($r_t = 132.1$ pc). If requiring the close meet distance smaller than 60 pc (like J0731+3717), only 3 mock stars are left. The result indicates that the high-velocity halo stars in our searching volume coincidentally insect with M15 by a pure chance of 1.2×10^{-5} (P_{orbit}). By an empirical cut on $V_\phi - [\text{Fe}/\text{H}]$ diagram (Figure S3), a total of 97,464 halo stars within the 5 kpc

searching volume are found from the existing large-scale spectroscopic surveys: SDSS DR12, LAMOST DR8, APOGEE DR16, and GALAH DR2. This means only 0.02 star could encounter with M15 within its tidal radius; but we indeed find one: the star J0731+3717.

Second, we estimate the possibility that stars possess chemical fingerprints similar to that of M15. To do so, a total of 1,930,135 stars (58,594 halo stars based on the aforementioned cut on V_ϕ -[Fe/H] diagram) with reliable determinations of [Fe/H] and $[\alpha/\text{Fe}]$ (requiring spectral SNR greater than 30) are selected from the existing large-scale spectroscopic surveys. Similar to the selection of high-velocity stars in ref.¹¹, all stars are within a 5 kpc searching volume by requiring parallax greater than 0.2 mas, parallax measurement error better than 20% and RUWE smaller than 1.4. Amongst these stars, 442 stars are found with [Fe/H] and $[\alpha/\text{Fe}]$ close to these of M15 within two times observational uncertainties of the cluster (see magenta box at Figure 2b). The values of [Fe/H] and $[\alpha/\text{Fe}]$ and their uncertainties of M15 are listed in Table 1. Therefore, 0.75% halo stars (442/58,594; P_{chem}) in our searching volume have similar chemical pattern on [Fe/H]- $[\alpha/\text{Fe}]$ as these of M15.

Finally, we check the age differences for those halo stars with chemical pattern similar to that of M15. The distances from *Gaia* DR3 parallax measurements¹¹ and SDSS *gri* photometric observations⁶ are cross-matched to those 442 aforementioned stars. By requiring photometric uncertainties smaller than 0.05 mag, 379 stars are left and shown in Figure 2c (grey diamonds). 62.8% of them (238/379; P_{CMD}) fall into the region within the two dashed magenta lines in Figure 2c and thus they have similar age as that of M15.

Overall, there is only 5.89×10^{-8} ($P_{\text{orbit}} \times P_{\text{chem}} \times P_{\text{CMD}}$) chance that J0731+3717 is not physically linked to M15. We thus conclude that J0731+3717 is ejected from M15 at a confidence level of “seven nines”.

I Black hole mass of M15.

By applying Hills mechanism to globular cluster, the most probable ejection velocity for a star is (ref.⁴¹),

$$v_{\text{ej}} \approx 460 \left(\frac{a}{0.1 \text{AU}} \right)^{-1/2} \left(\frac{m}{2M_\odot} \right)^{1/3} \left(\frac{M}{10^3 M_\odot} \right)^{1/6} \text{ km s}^{-1}, \quad (\text{S7})$$

where a is binary semimajor axis, m is the total mass of the binary and M is the mass of the massive black hole in the globular cluster. According to the momentum conservation, the ejection speeds for the primary and secondary are,

$$v_1 = v_{\text{ej}} \left(\frac{2m_2}{m} \right)^{1/2}, \text{ and } v_2 = v_{\text{ej}} \left(\frac{2m_1}{m} \right)^{1/2}, \quad (\text{S8})$$

respectively. m_1 and m_2 is the mass of primary and secondary. Following ref.⁴², the possibility of an ejection is expressed as,

$$P_{\text{ej}} = 1 - D/175, \quad (\text{S9})$$

where D is a dimensionless quantity,

$$D = \left(\frac{r_{\text{close}}}{a} \right) \left[\frac{2M}{10^6(m_1 + m_2)} \right]^{-1/3}. \quad (\text{S10})$$

Here r_{close} represents the closest distance that the binary can approach to the black hole of the cluster. $P_{\text{ej}} \equiv 0$ when $D > 175$.

As shown in the Fig. S2, the maximum mass of ‘undead’ star in the old cluster M15 is no greater than $1 M_\odot$. Even considering white dwarf with a mass close to Chandrasekhar limit as the companion, the mass ratio of the progenitor binary of J0731+3717 is no greater than 2. The mass ratio q is then assumed to uniformly distribute from 0 to 2. The mass of m_1 is equal to qm_2 , where m_2 denotes the mass of J0731+3717. For the binary semimajor axis, we adopt the present-day distribution (with age up to 13.6 Gyr; <https://cmc.ciera.northwestern.edu/home/>) for main-sequence binaries from the Cluster Monte Carlo (CMC) N -body simulations⁴³. Amongst the 148 independent N -body simulations, the model N16-RV0.5-RG8-Z0.1 was chosen since its present-day properties (e.g., a central velocity dispersion of 9.25 km s^{-1} and a half-mass radius of 3.9 pc at 13.6 Gyr) are very similar to these of M15 (a central velocity dispersion of 13.1 km s^{-1} and a half-mass radius of 3.66 pc; ref.⁴⁴, the last update can also found at <https://people.smp.uq.edu.au/HolgerBaumgardt/globular/parameter.html>). As same as ref.⁴¹, r_{close} is assumed to uniformly distribute between 0.1 and 700 AU. Finally, considering above assumptions and the observational constraints from the ejection velocity and stellar mass, as well as their uncertainties, of J0731+3717, we generate over 200 million progenitor binaries in the MC simulations to derive the mass distribution function of the black hole. By requiring $P_{\text{ej}} > 0$ and BH mass smaller than $10,000 M_\odot$ (3σ upper limit of the central dynamic mass within M15 found by previous studies^{45,46}), we find that the black hole mass of M15 is greater than $100 M_\odot$ with a credibility of 97.784%. Moreover, the closest distance r_{close} between the binary and black hole is largely (93.017%) within 2 AU, as the ejection probability decreases rapidly with increasing r_{close} (See Fig 3 and Fig. S4 for comparison). Our comprehensive analysis strongly suggests that J0731+3717 is ejected by an IMBH hosted by M15.

Finally, we remark that we can not fully rule out close encounters happened in some rare systems, for example, a single star scattered by binary IMBHs⁴⁷. These systems are of particular interesting for various astrophysical studies but obviously far beyond the current knowledge.

J Estimate the number of J0731+3717 like star in the searching volume of current and future surveys.

The current searching volume is limited by the *Gaia* DR3 parallax measurement that is only accurate for estimating stars with distance smaller than 5 kpc (ref.¹¹). For future *Gaia* DR5, the volume will be significantly expanded with distance as far as 10 kpc. We here attempt to estimate the number of J0731+3717 like star ejected from globular cluster via Hills mechanism in current and future searching volume. Doing so, we calculate mean ejection rate for 145 well known globular clusters in the full loss-cone and empty loss-cone regimes⁴⁸:

$$\mathcal{R}_{\text{full}} = f_b \left(\frac{a}{0.1 \text{AU}} \right) \left(\frac{n}{10^5 \text{pc}^3} \right) \left(\frac{M}{10^3 M_\odot} \right)^{4/3} \text{Myr}^{-1}, \quad (\text{S11})$$

and

$$\mathcal{R}_{\text{empty}} = f_b \left(\frac{n}{10^5 \text{pc}^3} \right)^2 \left(\frac{M}{10^3 M_\odot} \right)^3 \left(\frac{\sigma}{10 \text{kms}^{-1}} \right)^{-9} \text{Myr}^{-1}. \quad (\text{S12})$$

Here, we set cluster binary fraction $f_b = 8.8\%$ (ref.⁴⁹), and a constant binary separation of 0.05 AU. The central stellar number density n is estimated by the cluster central mass density and typical mass of a star in globular cluster. The former can be found at <https://people.smp.uq.edu.au/HolgerBaumgardt/globular/parameter.html> and the latter is assumed to be $0.8 M_\odot$. M is the mass of central black hole which is extrapolated from M - σ relation⁵⁰. σ is the cluster central velocity dispersion that can again be found at <https://people.smp.uq.edu.au/HolgerBaumgardt/globular/parameter.html>. The number of recent ejections for each cluster can thus be calculated by $N_{\text{ej}} = \bar{\mathcal{R}} \Delta T$ in the past 250 Myr (i.e. $\Delta T = 250 \text{ Myr}$). $\bar{\mathcal{R}}$ is the mean of $\mathcal{R}_{\text{full}}$ and $\mathcal{R}_{\text{empty}}$. On average, the ejection rate is 1.34 Myr^{-1} for a cluster. We then run MC simulations to perform the ejection experiments. In each simulation, all the orbits of 145 globular cluster are integrated back to 250 Myr with a time resolution of 0.1 Myr, N_{ej} ejection events for each cluster are thus uniformly distributed in past 250 Myr. For each event, a star is assumed to be kicked off from the cluster isotropically by a velocity v_{ej} , which can be calculated from Equations 7 and 8 by assuming a binary containing two J0731+3717 like stars with a constant separation of 0.05 AU. All these ejected stars are then integrated to present-day. In total, we performed 100 MC simulations. On average, over thirty thousand J0731+3717 like high-velocity stars with $V_{\text{GSR}} \geq 400 \text{ km s}^{-1}$ are kicked off from clusters, corresponding to an ejection rate of around 10^{-4} yr^{-1} , which is well consistent with that estimated from a dynamical numerical simulation (ref.⁵²). As a comparison, only 10 such high-velocity stars, ejected in the past 250 Myr are found in the Monte Carlo N -body simulations (<https://zenodo.org/record/7599871>) for single-binary interaction involving compact objects by ref.⁵¹. Its rate, about $4 \times 10^{-8} \text{ yr}^{-1}$, is three orders of magnitude lower than that of Hills mechanism we consider here. In our simulations, the number of J0731+3717 like stars within 5 and 10 kpc from the Sun are found to be 49_{-7}^{+7} and 480_{-32}^{+48} , respectively. The values and uncertainties are given by the PDF generated by 100 MC simulations. If we consider the past 14 Gyr (the age of universe) instead of the above 250 Myr, the number of ejected stars within 5 kpc from the Sun is 537_{-27}^{+24} (without considerations of dynamical effects). This result shows that the current searching volume potentially contains a large number of high-velocity stars ejected from globular clusters but their orbits are difficult to be linked to their host clusters since most of them are not ejected recently. We note that all the above simulation results are based on a series of parameters from previous studies, which may still be under debate. However, the predicted order of magnitude is meaningful.

Currently, we have found one of the nearly hundred cluster ejected high-velocity stars as predicted by our above MC simulations. We expect dozens of more such star(s) can be discovered in the near future, with the fast increasing sampling rate of large-scale spectroscopic surveys (e.g., the LAMOST, SDSS-V and DESI). With the final release of *Gaia* DR5, the number can be even increased to a factor of ten, more details about the IMBHs hosted by globular clusters can be explored at that time.

Table S1: Top 5 globular clusters sorted by the ratio of the closest orbital distance to the clusters' tidal radius (from small to large) in the backward orbital analysis of J0731+3717.

Cluster name	Closest distance (d_{min}) (kpc)	Backward time (Myr)	Tidal radius (r_t) (kpc)	d_{min}/r_t
M15	0.058	21.1	0.132	0.44
Pal 10	2.779	16.3	0.063	43.85
NGC 6715	12.867	46.9	0.279	46.09
NGC 7089	5.813	17.5	0.111	52.47
NGC 6121	2.845	1.7	0.054	52.74

Reference

- GRAVITY Collaboration, Abuter, R., Amorim, A., et al. 2019, *Astron. Astrophys.*, 625, L10. doi:10.1051/0004-6361/201935656
- Bland-Hawthorn, J. & Gerhard, O. 2016, *ARA&A*, 54, 529. doi:10.1146/annurev-astro-081915-023441

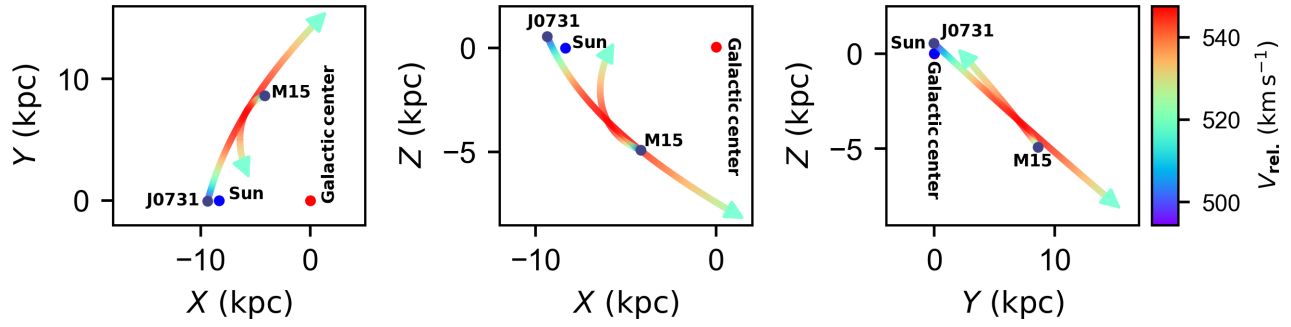


Figure S1: The 3D backward orbits of J0731+3717 and M15 projected in X–Y (left), X–Z (middle) and Y–Z (right) planes, color coded by the relative velocity between each other as indicated by the right colorbar. The positions of the Galactic center and the Sun are represented by the red and blue dots, respectively.

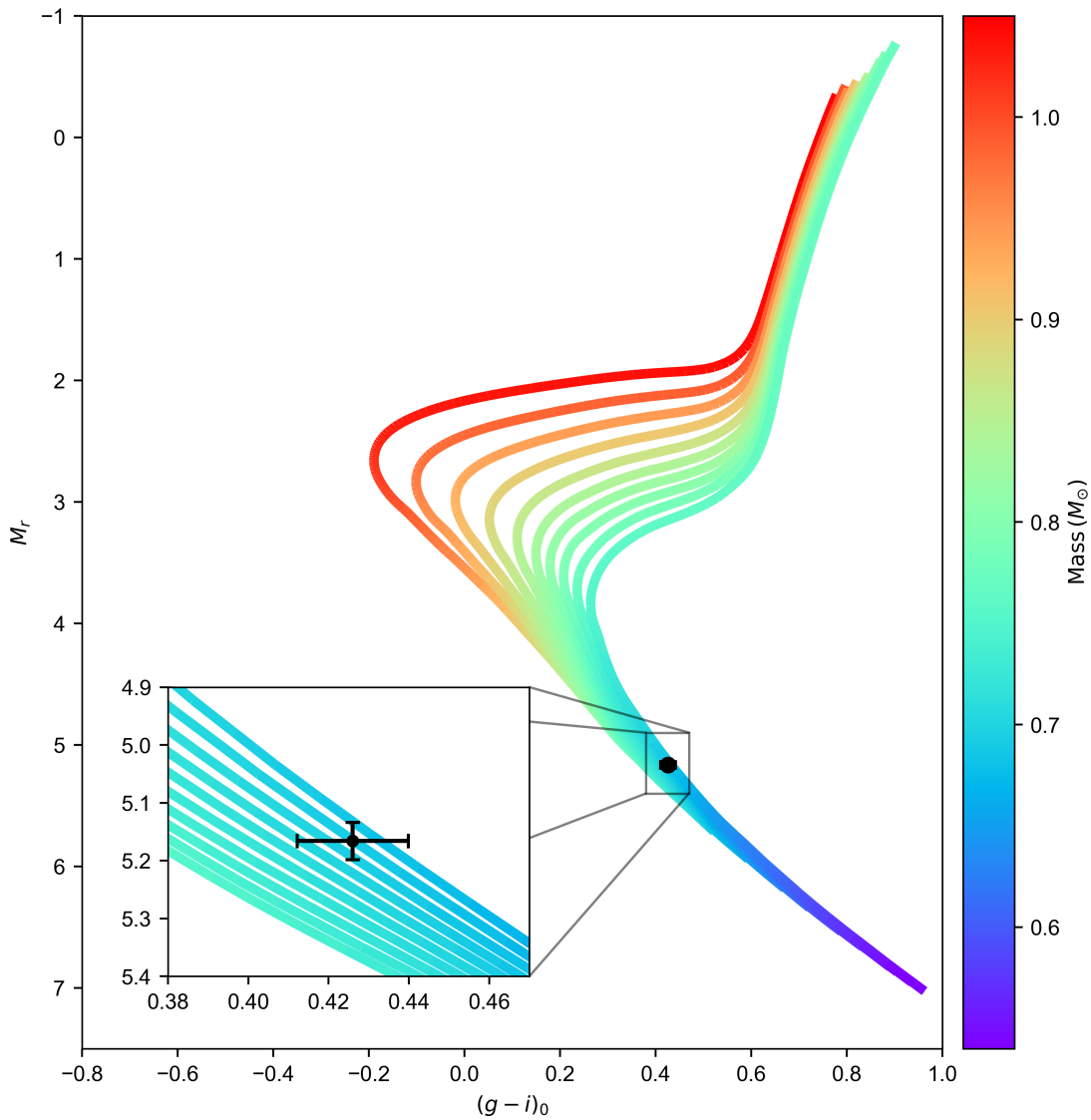


Figure S2: Comparison of J0731+3717 and stellar isochrones on $(g - i)_0$ versus M_r diagram. The black dot with error bar marks the position of J0731+3717. The background shows ten isochrones with ages ranging from 5 to 14 Gyr in a step of 1 Gyr (left to right) taken from DSEP. The colors represent the stellar mass, as indicated by the right color bar. All the isochrones have constant $[\text{Fe}/\text{H}]$ of -2.23 and $[\alpha/\text{Fe}]$ of $+0.20$. Zoom inset shows the comparison more clearly.

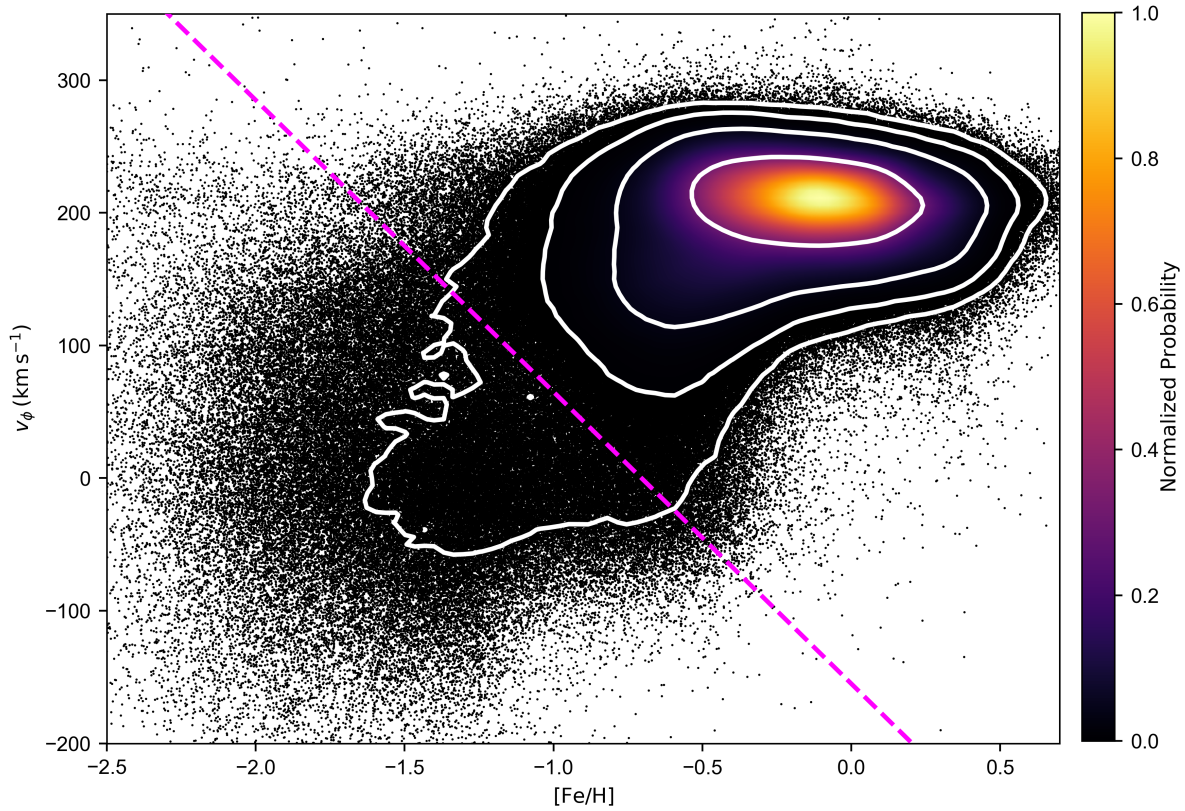


Figure S3: The density distribution of v_ϕ vs. $[\text{Fe}/\text{H}]$ for 5,020,788 stars observed by SDSS DR12, LAMOST DR8, APOGEE DR16, and GALAH DR2 with spectral signal-to-noise ratio greater than 10. Similar to ref.¹¹, all stars are required to have parallax greater than 0.2 mas, parallax measurement uncertainty better than 20% and RUWE smaller than 1.4. The magenta dashed-line is an empirical cut to separate the disk population (upper right) and halo population (lower left).

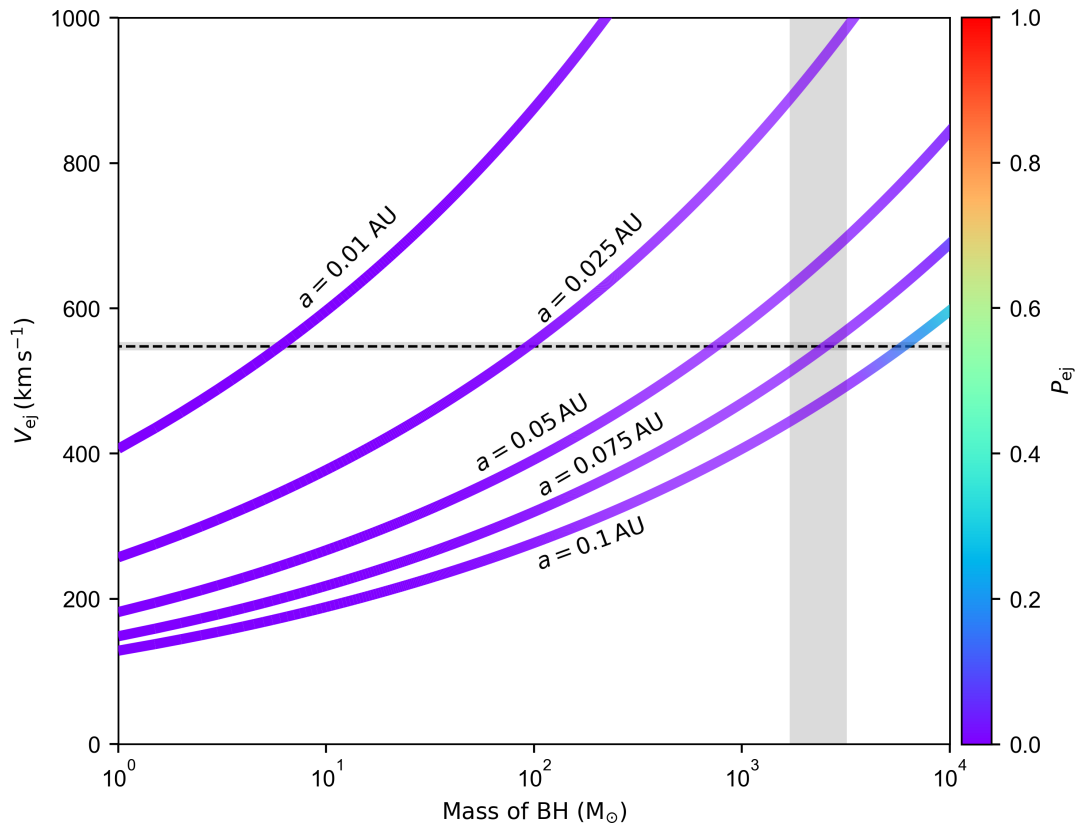


Figure S4: Ejection velocities predicted by Hills mechanism. This plot resembles Fig. 3, but with the closest distance between the binary and the black hole set to 3 AU. The ejection probability, as indicated by the colorbar on the right side, is almost zero for most black hole masses and binary separation configurations.

Table S2: Backward orbital results under different assumptions.

Changed assumptions	Closest orbital distance	Backward time
	(pc)	(Myr)
BovyMWPotential2014	56.3	21.3
$(U_{\odot}, V_{\odot}, W_{\odot}) = (11.10, 12.24, 7.25) \text{ km s}^{-1}$	57.8	21.1
$V_c(R_0) = 234.04 \text{ km s}^{-1}$	59.1	21.1
$R_0 = 8.34 \text{ kpc}$	53.1	21.1
Modelling M15 as a moving Plummer potential	55.6	21.1
Adding potential from LMC	50.9	21.1

3. Bovy, J. 2015, *Astrophys. J. Supp.*, 216, 29. doi:10.1088/0067-0049/216/2/29
4. Huang, Y., Liu, X.-W., Yuan, H.-B., et al. 2015, *Mon. Not. R. Astron. Soc.*, 449, 162. doi:10.1093/mnras/stv204
5. Kunder, A., Kordopatis, G., Steinmetz, M., et al. 2017, *Astron. J.*, 153, 75. doi:10.3847/1538-3881/153/2/75
6. Alam, S., Albaret, F. D., Allende Prieto, C., et al. 2015, *Astrophys. J. Supp.*, 219, 12. doi:10.1088/0067-0049/219/1/12
7. Luo, A.-L., Zhao, Y.-H., Zhao, G., et al. 2015, *Research in Astronomy and Astrophysics*, 15, 1095. doi:10.1088/1674-4527/15/8/002
8. Jönsson, H., Holtzman, J. A., Allende Prieto, C., et al. 2020, *Astron. J.*, 160, 120. doi:10.3847/1538-3881/aba592
9. Buder, S., Asplund, M., Duong, L., et al. 2018, *Mon. Not. R. Astron. Soc.*, 478, 4513. doi:10.1093/mnras/sty1281
10. Gaia Collaboration, Vallenari, A., Brown, A. G. A., et al. 2023, *Astron. Astrophys.*, 674, A1. doi:10.1051/0004-6361/202243940
11. Li, Q.-Z., Huang, Y., Dong, X.-B., et al. 2023, *Astron. J.*, 166, 12. doi:10.3847/1538-3881/acd1dc
12. Xiang, M. S., Liu, X. W., Yuan, H. B., et al. 2015, *Mon. Not. R. Astron. Soc.*, 448, 822. doi:10.1093/mnras/stu2692
13. Price-Whelan, A. M. 2017, *The Journal of Open Source Software*, 2, 388. doi:10.21105/joss.00388
14. Chandrasekhar, S. 1943, *Astrophys. J.*, 97, 255. doi:10.1086/144517
15. Fritz, T. K., Battaglia, G., Pawlowski, M. S., et al. 2018, *Astron. Astrophys.*, 619, A103. doi:10.1051/0004-6361/201833343
16. Binney, J. & Tremaine, S. 2008, *Galactic Dynamics: Second Edition*, by James Binney and Scott Tremaine. ISBN 978-0-691-13026-2 (HB). Published by Princeton University Press, Princeton, NJ USA, 2008.
17. Bailer-Jones, C. A. L., Rybizki, J., Andrae, R., et al. 2018, *Astron. Astrophys.*, 616, A37. doi:10.1051/0004-6361/201833456
18. Schönrich, R., Binney, J., & Dehnen, W. 2010, *Mon. Not. R. Astron. Soc.*, 403, 1829. doi:10.1111/j.1365-2966.2010.16253.x
19. Zhou, Y., Li, X., Huang, Y., et al. 2023, *Astrophys. J.*, 946, 73. doi:10.3847/1538-4357/acadd9
20. Reid, M. J., Menten, K. M., Brunthaler, A., et al. 2014, *Astrophys. J.*, 783, 130. doi:10.1088/0004-637X/783/2/130
21. Harris, W. E. 2010, arXiv:1012.3224. doi:10.48550/arXiv.1012.3224
22. Vasiliev, E. & Baumgardt, H. 2021, *Mon. Not. R. Astron. Soc.*, 505, 5978. doi:10.1093/mnras/stab1475
23. Baumgardt, H. & Vasiliev, E. 2021, *Mon. Not. R. Astron. Soc.*, 505, 5957. doi:10.1093/mnras/stab1474
24. Erkal, D., Belokurov, V., Laporte, C. F. P., et al. 2019, *Mon. Not. R. Astron. Soc.*, 487, 2685. doi:10.1093/mnras/stz1371
25. Patel, E., Kallivayalil, N., Garavito-Camargo, N., et al. 2020, *Astrophys. J.*, 893, 121. doi:10.3847/1538-4357/ab7b75
26. Yanny, B., Rockosi, C., Newberg, H. J., et al. 2009, *Astron. J.*, 137, 4377. doi:10.1088/0004-6256/137/5/4377
27. Lee, Y. S., Beers, T. C., Sivarani, T., et al. 2008, *Astron. J.*, 136, 2022. doi:10.1088/0004-6256/136/5/2022
28. Lee, Y. S., Beers, T. C., Sivarani, T., et al. 2008, *Astron. J.*, 136, 2050. doi:10.1088/0004-6256/136/5/2050
29. Husser, T.-O., Wende-von Berg, S., Dreizler, S., et al. 2013, *Astron. Astrophys.*, 553, A6. doi:10.1051/0004-6361/201219058
30. Prugniel, P. & Soubiran, C. 2001, *Astron. Astrophys.*, 369, 1048. doi:10.1051/0004-6361:20010163
31. Adelman-McCarthy, J. K., Agüeros, M. A., Allam, S. S., et al. 2008, *Astrophys. J. Supp.*, 175, 297. doi:10.1086/524984
32. Salpeter, E. E. 1955, *Astrophys. J.*, 121, 161. doi:10.1086/145971
33. Dotter, A., Chaboyer, B., Jevremović, D., et al. 2008, *Astrophys. J. Supp.*, 178, 89. doi:10.1086/589654
34. Schlegel, D. J., Finkbeiner, D. P., & Davis, M. 1998, *Astrophys. J.*, 500, 525. doi:10.1086/305772
35. Yuan, H. B., Liu, X. W., & Xiang, M. S. 2013, *Mon. Not. R. Astron. Soc.*, 430, 2188. doi:10.1093/mnras/stt039
36. An, D., Johnson, J. A., Clem, J. L., et al. 2008, *Astrophys. J. Supp.*, 179, 326. doi:10.1086/592090
37. Stetson, P. B. 1987, *PASP*, 99, 191. doi:10.1086/131977
38. Stetson, P. B. 1994, *PASP*, 106, 250. doi:10.1086/133378
39. Sandage, A., Katem, B., & Sandage, M. 1981, *Astrophys. J. Supp.*, 46, 41. doi:10.1086/190734
40. Anguiano, B., Majewski, S. R., Hayes, C. R., et al. 2020, *Astron. J.*, 160, 43. doi:10.3847/1538-3881/ab9813
41. Bromley, B. C., Kenyon, S. J., Geller, M. J., et al. 2006, *Astrophys. J.*, 653, 1194. doi:10.1086/508419
42. Hills, J. G. 1988, *Nature*, 331, 687. doi:10.1038/331687a0
43. Kremer, K., Ye, C. S., Rui, N. Z., et al. 2020, *Astrophys. J. Supp.*, 247, 48. doi:10.3847/1538-4365/ab7919
44. Baumgardt, H. & Hilker, M. 2018, *Mon. Not. R. Astron. Soc.*, 478, 1520. doi:10.1093/mnras/sty1057
45. Gerssen, J., van der Marel, R. P., Gebhardt, K., et al. 2002, *Astron. J.*, 124, 3270. doi:10.1086/344584
46. Gerssen, J., van der Marel, R. P., Gebhardt, K., et al. 2003, *Astron. J.*, 125. doi:10.1086/345574
47. Fragione, G. & Bromberg, O. 2019, *Mon. Not. R. Astron. Soc.*, 488, 4370. doi:10.1093/mnras/stz2024
48. Šubr, L., Fragione, G., & Dabringhausen, J. 2019, *Mon. Not. R. Astron. Soc.*, 484, 2974. doi:10.1093/mnras/stz162
49. Ji, J. & Bregman, J. N. 2015, *Astrophys. J.*, 807, 32. doi:10.1088/0004-637X/807/1/32
50. Gültekin, K., Richstone, D. O., Gebhardt, K., et al. 2009, *Astrophys. J.*, 698, 198. doi:10.1088/0004-637X/698/1/198
51. Cabrera, T. & Rodriguez, C. L. 2023, *Astrophys. J.*, 953, 19. doi:10.3847/1538-4357/acdc22
52. Fragione, G. & Gualandris, A. 2019, *Mon. Not. R. Astron. Soc.*, 489, 4543. doi:10.1093/mnras/stz2451